

Nonvolatile multiple-valued memory device using lateral spin valve

Kimura, Takashi

Advanced Electronics Research Division, INAMORI Frontier Research Center, Kyushu University

Hara, Makoto

Graduate School of Science and Technology, Kumamoto University

<https://hdl.handle.net/2324/26355>

出版情報 : Applied Physics Letters. 97 (18), pp.182501(1)-182501(3), 2010-11-01. American Institute of Physics

バージョン :

権利関係 : (C) 2010 American Institute of Physics



Nonvolatile multiple-valued memory device using lateral spin valve

T. Kimura and M. Hara

Citation: *Appl. Phys. Lett.* **97**, 182501 (2010); doi: 10.1063/1.3502475

View online: <http://dx.doi.org/10.1063/1.3502475>

View Table of Contents: <http://apl.aip.org/resource/1/APPLAB/v97/i18>

Published by the American Institute of Physics.

Related Articles

Stress reconfigurable tunable magnetoelectric resonators as magnetic sensors

Appl. Phys. Lett. **102**, 042909 (2013)

Electrical control of magnetic reversal processes in magnetostrictive structures

Appl. Phys. Lett. **102**, 032405 (2013)

Precessional reversal in orthogonal spin transfer magnetic random access memory devices

Appl. Phys. Lett. **101**, 032403 (2012)

Hot spin-wave resonators and scatterers

J. Appl. Phys. **112**, 013902 (2012)

Magnetic domain wall transfer via graphene mediated electrostatic control

Appl. Phys. Lett. **101**, 013103 (2012)

Additional information on *Appl. Phys. Lett.*

Journal Homepage: <http://apl.aip.org/>

Journal Information: http://apl.aip.org/about/about_the_journal

Top downloads: http://apl.aip.org/features/most_downloaded

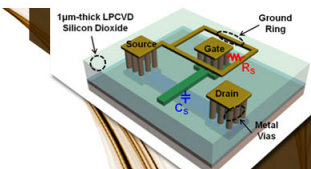
Information for Authors: <http://apl.aip.org/authors>

ADVERTISEMENT

AIP | Applied Physics
Letters

**EXPLORE WHAT'S
NEW IN APL**

SUBMIT YOUR PAPER NOW!



**SURFACES AND
INTERFACES**

Focusing on physical, chemical, biological, structural, optical, magnetic and electrical properties of surfaces and interfaces, and more...

**ENERGY CONVERSION
AND STORAGE**

Focusing on all aspects of static and dynamic energy conversion, energy storage, photovoltaics, solar fuels, batteries, capacitors, thermoelectrics, and more...

Nonvolatile multiple-valued memory device using lateral spin valve

T. Kimura^{1,a)} and M. Hara²

¹Advanced Electronics Research Division, INAMORI Frontier Research Center, Kyushu University, 744 Motoooka, Fukuoka 819-0395, Japan

²Graduate School of Science and Technology, Kumamoto University, 2-39-1 Kurokami, Kumamoto 860-8555, Japan

(Received 24 July 2010; accepted 26 September 2010; published online 1 November 2010)

The authors propose a nonvolatile multiple-valued memory based on a nonlocal spin valve structure. Multibit informations are formed by changing the magnetization configuration in a nonlocal voltage probe consisting of a magnetic multilayer. A simple calculation method for the spin-accumulation voltage induced in lateral ferromagnetic/nonmagnetic multilayered hybrid structures is also developed on the basis of the spin resistance model. The developed model enables us to find the thickness of each ferromagnetic layer for the optimized operation of the multiple-valued memory.

© 2010 American Institute of Physics. [doi:10.1063/1.3502475]

Nanostructured spintronic devices such as magnetic and spin random access memories (RAMs) are promising candidates for future nonvolatile memories and storage devices because of their high performances.^{1,2} Especially, high speed operation and unlimited endurance are great advantages of the spintronic devices compared to other nonvolatile memories such as flash memory and ferroelectric RAM. Recent developments of the nanofabrication technique in spintronic devices achieve a tiny magnetic cell with a lateral dimension down to 100 nm. In order to realize a high density RAM over 10 Gbit/cm², a further reduction in the magnetic element size (~ 50 nm) is required. However, the magnetizations in such nanostructures become unstable because of the thermal fluctuation.³ Thus, the areal density of the magnetic devices is limited by the thermal stability of the magnetizations.

A conventional magnetic devices store one bit information in a single memory cell. When two or more bit informations can be stored in one unit cell, the areal density drastically increases without reducing the lateral dimension. This is known as multiple-valued logic (MVL) devices, which are mainly developed in floating-gate metal oxide semiconductor transistors.⁴ MVL is a promising approach for future massive data storage devices and realizes more functional devices than the binary logic devices. Since the spintronic devices operate much faster than the conventional floating-gate-type MVL devices, a creation of the spin-based nonvolatile MVL opens up new aspects of spintronic devices. Here, we propose a multiple-valued nonvolatile memory based on the ferromagnetic nanostructures.

We use a nonlocal spin injection and detection techniques in a lateral ferromagnetic (F)/nonmagnetic (N) hybrid structure to realize a nonvolatile multiple-valued memory.⁵⁻⁹ In the vertical structure, a large background signal induced by the local charge current makes it difficult to distinguish several intermediate states. On the other hand, in nonlocal spin valve measurements, the spin-related signal is sensitively detected by a nonlocal ferromagnetic voltage probe without spurious background signals. The induced voltage depends on the relative magnetization orientation between the injector and detector. Thus, the conventional lat-

eral spin valve can store one bit information. In the present paper, we propose a multiple-valued memory based on a lateral spin valve structure with the ferromagnetic voltage probe consisting ferromagnetic/nonmagnetic multilayers.

A schematic illustration of the proposed device is shown in Fig. 1. The device is composed of a ferromagnetic spin injector Fi, a nonmagnetic strip N0 and a multiple-valued memory element consisting of a F/N/F trilayer structure. The detailed structure of the F/N/F trilayer is shown in the right-hand side of Fig. 1. Here, F1 and F3 are the first and second ferromagnetic layers, respectively. N2 is the nonmagnetic spacer with the thickness d_1 . The thickness d_1 for F1 is comparable to λ_{F1} while d_{F3} for F3 is much thicker than λ_3 . The thickness d_2 is much thinner than λ_2 . Here, λ_1 , λ_2 and λ_3 are the spin diffusion lengths for F1, N2, and F3, respectively. The magnetizations for F1 and F3 can be controlled by the Oersted field induced by flowing the current in the nonmagnetic strip as schematically shown in Fig. 1 or nonlocal spin current injection.^{10,11} The magnetization of the spin injector Fi should be fixed during the operation.

First, we calculate the spin accumulation $\Delta\mu = \mu_{\uparrow} - \mu_{\downarrow}$ induced in the nonmagnetic strip N0, where μ_{\uparrow} and μ_{\downarrow} are the spin-dependent chemical potentials for up and down spins, respectively. For the calculation, we extend the spin resistance model developed in Ref. 12 to magnetic-multilayered detectors. Using the spin resistances for the injector R_{SFi} and the effective spin resistance for detector R_{SE1} , one can easily calculate the nonlocal spin accumulation $\Delta\mu_1$

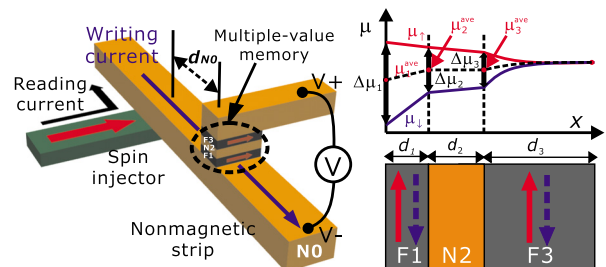


FIG. 1. (Color online) Schematic illustration of a proposed nonvolatile multiple-valued memory based on a lateral spin valve structure and the detailed of the $F_1/N_2/F_3$ trilayer memory element for 2-bit storage together with the spin-dependent chemical potential induced by nonlocal spin accumulation. A dotted line shows a spatial distribution of μ_{ave} .

^{a)}Electronic mail: kimura@ifrc.kyushu-u.ac.jp.

induced at the junction between the nonmagnetic strip N0 and F1 under the injection current I_C as¹²⁻¹⁴

$$\Delta\mu_1 = \frac{eP_{Fi}I_C R_{S0}}{\left(2 + \frac{R_{S0}(R_{SFi} + R_{SE1})}{R_{SFi}R_{SE1}}\right)e\frac{d_0}{\lambda_0} + \frac{R_{S0}^2 \sinh(d_0/\lambda_0)}{R_{SFi}R_{SE1}}}, \quad (1)$$

P_{Fi} and d_0 are, respectively, the spin polarization of the spin injector Fi and the distance between the injector and detector. R_{S0} and λ_0 are, respectively, the spin resistance and the spin diffusion length for the nonmagnetic strip N0. The spin resistance for homogeneous materials is simply defined by $2\rho\lambda/[(1-P^2)S]$, where ρ , λ , P , and S are, respectively, the resistivity, spin diffusion length, spin polarization, and effective cross section for the spin current. When the material connects an different material, the spin resistance is modified from the homogeneous case. The effective spin resistance for inhomogeneous structure such as the multi terminals or multilayers can be expressed by the series and parallel connections of the spin resistance.¹² Since the detector of the present device consists of the F1/N2/F3 trilayer, the effective spin resistance R_{SE1} for the detector can be calculated as $R_{S1}[R_{S1} \sinh(d_1/\lambda_1) + R_{SE2} \cosh(d_1/\lambda_1)]/[R_{S1} \times \cosh(d_1/\lambda_1) + R_{SE2} \sinh(d_1/\lambda_1)]$. Here, R_{S1} is the spin resistances for F1. R_{SE2} is the effective spin resistance for the series connection of N2 and F3 and is given by $R_{S2}[R_{S2} \sinh(d_2/\lambda_2) + R_{S3} \cosh(d_2/\lambda_2)]/[R_{S2} \cosh(d_2/\lambda_2) + R_{S3} \sinh(d_2/\lambda_2)]$. Here, R_{S2} and R_{S3} are the spin resistances for N2 and F3, respectively.

As in the above equation, the spin accumulation $\Delta\mu_1$ is independent of the magnetization directions for F1 and F3. $\Delta\mu_1$ decreases to $\Delta\mu_2$ at the interface between F1 and N2 because of the spin relaxation in the F1. We define the attenuation constant T_1 as $\Delta\mu_2/\Delta\mu_1$. Using the spin resistance model, T_1 can be calculated as $R_{SE2}/[R_{S1} \sinh(d_1/\lambda_1) + R_{SE2} \cosh(d_1/\lambda_1)]$. It should be noted that the attenuation constant T_1 is also independent of the magnetization directions for F1 and F3.

We then calculate the averaged electrochemical potential μ^{ave} defined by $(\mu_1 + \mu_2)/2$. μ^{ave} corresponds to the detecting electrostatic potential after the spin relaxation ($\Delta\mu=0$). Since μ_1 and μ_2 symmetrically decay in nonmagnets, μ^{ave} is not modified in nonmagnets. However, μ^{ave} is modified in ferromagnets because the conductivity depends on the spin direction. In the present case, μ_1^{ave} at the interface between the N0 and F1 changes to μ_2^{ave} at the interface between F1 and N2. The chemical potential shift $\Delta\mu_1^S$, which is the difference in between μ_1^{ave} and μ_2^{ave} , is given by

$$\Delta\mu_1^S \equiv \mu_2^{ave} - \mu_1^{ave} = [\alpha_1(1 - T_1)/2]\Delta\mu_0 = S_1\Delta\mu_0. \quad (2)$$

α_1 is the up-spin polarization defined as $(\sigma_{1\uparrow} - \sigma_{1\downarrow})/(\sigma_{1\uparrow} + \sigma_{1\downarrow})$, where $\sigma_{1\uparrow}$ and $\sigma_{1\downarrow}$ are the electrical conductivity for up and down spins, respectively. When the magnetization of F1 is parallel (antiparallel) to the spin injector Fi, α_1 is positive (negative). Thus, $\Delta\mu_1^S$ depends on the magnetization direction of F1. This corresponds to the fact that the induced nonlocal voltage in the lateral spin valve depends on the relative magnetization configuration of the injector and detector. S_1 is the shift constant defined by $\Delta\mu_1^S/\Delta\mu_0$, and is given by $\alpha_1(1 - T_1)/2$. When d_1 is much thicker than λ_1 , S_1 becomes $\alpha_1/2$. This corresponding to the nonlocal voltage induced in the conventional lateral spin valve. However

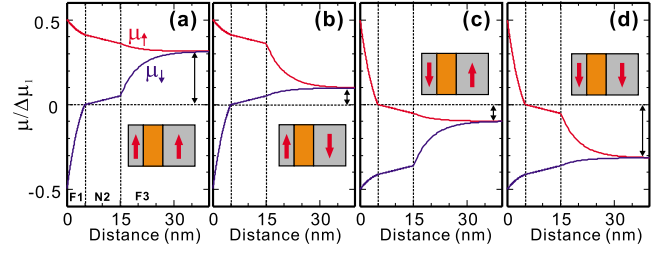


FIG. 2. (Color online) Calculated spin-dependent electro-chemical potentials μ_1 and μ_2 for four magnetization configurations in the F1/N2/F3 trilayer voltage probe.

when d_1 is not so thick, S_1 becomes smaller than $\alpha_1/2$.

As in Fig. 1(b), in the trilayer detector, the voltage V generated in the voltage meter is given by $(\Delta\mu_1^S + \Delta\mu_2^S + \Delta\mu_3^S)/e$. Here, the second term $\Delta\mu_2^S$ is zero because N2 does not induce the change in $\Delta\mu_{ave}$. Therefore the observed voltage V_{2bit} is given by

$$V_{2bit} = (S_1\Delta\mu_0 + S_3\Delta\mu_2)/e = (S_1 + T_1T_2S_3)(\Delta\mu_0/e). \quad (3)$$

T_2 is the attenuation constant due to the spin relaxation of N1 and is given by $R_{S3}/[R_{S2} \sinh(d_2/\lambda_2) + R_{S3} \cosh(d_2/\lambda_2)]$. S_3 is the shift constant due to F3. Since F3 is much thicker than λ_3 , S_3 is simply given by $\alpha_3/2$, where α_3 is the up-spin polarization defined similar to α_1 . There are four magnetization configurations for F1 and F3 ($\uparrow\uparrow, \uparrow\downarrow, \downarrow\uparrow, \downarrow\downarrow$). Each configuration induces the different voltage. Therefore, the present device operates as a 2-bit memory.

For the best operation of 2-bit memory, the voltage difference ΔV between neighboring spin states should be the same as in the following relation: $\Delta V = V_{\uparrow\uparrow} - V_{\uparrow\downarrow} = V_{\uparrow\downarrow} - V_{\downarrow\downarrow} = V_{\downarrow\downarrow} - V_{\downarrow\uparrow}$. From Eq. (3), this condition is realized by satisfying $2T_1T_2S_3 = S_1$. As a realistic case, we consider a CoFe/Cu/CoFe trilayer. We assume that $d_2 = 0.02\lambda_{N2}$ since the spin diffusion length for Cu is typically submicron scale. Using the typical values of $\lambda_{Cu} = 500$ nm, $\lambda_{CoFe} = 5$ nm, $P_{CoFe} = 0.7$, and $R_{SCu} \approx 20R_{SCoFe}$, we obtain $d_{F1} \approx 1.02\lambda_{F1}$ for the best operation. Figure 2 shows the calculated electrochemical potentials μ_1 and μ_2 for the four different configurations at the best condition. The four different magnetization configurations clearly show four different voltages with the same interval ΔV_{int} . This means that the operation of the 2-bit memory is well optimized.

When the number of the ferromagnetic layers is m , the device can be extended to a multiple-valued memory with m bit informations. Here, the magnetization direction of n th ferromagnetic layer simply corresponds to the n th bit information. Since neighboring ferromagnetic layers are separated by a nonmagnetic spacer, the total number of the layers is $2m - 1$. Therefore, the induced voltage is simply obtained by

$$V = \frac{\Delta\mu_0}{e} \sum_{i=1}^{2m-1} S_i \prod_{j=1}^i T_{j-1}. \quad (4)$$

The attenuation constant T_{j-1} defined by $\Delta\mu_{j-1}/\Delta\mu_{j-2}$ is given by $R_{SEj}/[R_{Sj-1} \sinh(d_{j-1}/\lambda_{j-1}) + R_{SEj} \cosh(d_{j-1}/\lambda_{j-1})]$, with $T_0 = 1$, where, R_{SEj} is the effective spin resistance defined by $R_{Si}[R_{Si} \sinh(d_i/\lambda_i) + R_{SEi+1} \cosh(d_i/\lambda_i)]/[R_{Si} \cosh(d_i/\lambda_i) + R_{SEi+1} \sinh(d_i/\lambda_i)]$. The shift constant S_i is given by $S_i = \alpha_i(1 - T_i)/2$. It should be noted that the shift constant S_i is zero when the i th layer is non-magnet ($i = 2n$, n is integer).

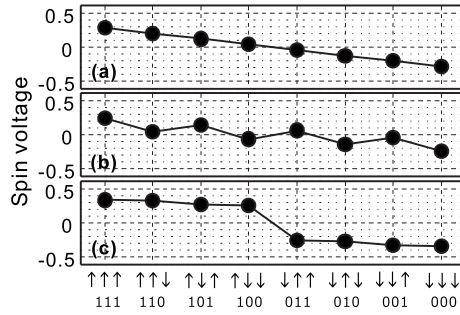


FIG. 3. Calculated voltages for different eight spin orientations in a 3-bit multiple nonlocal spin memory at (a) $d_{F1}=0.74\lambda_F$ and $d_{F3}=1.02\lambda_F$, (b) $d_{F1}=d_{F3}=0.4\lambda_F$, and (c) $d_{F1}=d_{F3}=5\lambda_F$.

Here, we consider a 3-bit device operation consisting of a F1/N2/F3/N4/F5 magnetic multilayer. We assume that F1 and F3 are the same ferromagnetic material with the thickness d_1 and d_3 , respectively. F5 is also the same ferromagnetic material but the thickness is much longer than the spin diffusion length λ_F . N2 and N4 are the same nonmagnetic materials with a same thickness d_N , where, N has a long spin diffusion length. From Eq. (4), the induced voltage V_{3bit} in the 3-bit device is expressed by

$$V_{3bit} = (S_1 + T_1 T_2 S_3 + T_1 T_2 T_3 T_4 S_5)(\Delta\mu_0/e). \quad (5)$$

As discussed before, to obtain the systematic voltage change in response to each spin configuration, the thickness of each layer in the multilayered voltage probe should be well optimized especially for the ferromagnetic layers F1 and F3 in the 3-bit device. Similarly in the 2-bit device, for the best operation, the voltage difference ΔV between neighboring spin states should be the same as in the following equation: $\Delta V = V_{\uparrow\uparrow\uparrow} - V_{\uparrow\uparrow\downarrow} = V_{\uparrow\uparrow\downarrow} - V_{\uparrow\downarrow\uparrow} = V_{\uparrow\downarrow\uparrow} - V_{\uparrow\downarrow\downarrow}$. From these relations, we obtain the relations $S_1 - T_1 T_2 S_3 = 2T_1 T_2 T_3 T_4 S_5$, and $S_3 = 2T_3 T_4 S_5$, for the best operation.

We calculate the induced voltage also in a realistic 3-bit device consisting of CoFe/Cu/CoFe/Cu/CoFe fifth multilayer. In the calculation, we use the same parameters in the 2-bit device. The best operation is realized by the condition $d_1=0.74\lambda_F$ and $d_3=1.02\lambda_F$. Figure 3(a) shows the voltage induced in the multibit device at the best condition. Clear multibit voltage states corresponding to the eight spin orientations have been obtained. However, the voltage does not change systematically when the F1 and F3 is too thin ($d_1=d_3=0.4\lambda_F$), as shown in Fig. 3(b). Moreover, as in Fig. 3(c), the multibit voltage states are not formed when d_1 is thicker than λ_F ($d_1=d_3=5\lambda_F$) because of the decay of the spin accumulation. Thus, the thickness for the ferromagnetic layer is one of the most important parameters.

Another important issue is how to obtain all of the magnetization configurations in the multibit devices, namely writing method. In the 2-bit device, each magnetization can be controlled simply by the magnetic field as in Fig. 1(a) because of the difference in the coercive fields. However, in the 3-bit or more multibit devices, it is difficult to control the magnetization configurations by adjusting the magnetic field. In a 3-bit device, dual spin injections from the top (F5) and bottom (F1) layers in the voltage probe can control each magnetization.^{10,11} By realizing the 3-bit device, the areal density increases by a factor of 9 from the conventional one

bit device. For realizing more multibit devices, one may solve the writing issue by combining the nonlocal spin injection with the magnetic field.

Conventional vertical structures consisting of F/N multilayers may also realize a similar multiple-valued memory. However, in vertical structures, the large background resistance due to the Ohmic voltage drop of the system makes it difficult to distinguish the multispin states. Moreover, the resistance mainly depends on the magnetization configuration between the neighboring ferromagnetic layers. For example, in a magnetic multilayer with three ferromagnetic layers, the configuration $\uparrow\uparrow\downarrow$ and $\downarrow\uparrow\uparrow$ do not induce a large difference in the local resistance such as the current-perpendicular-to-plane configuration.¹⁵ This makes it difficult to distinguish the multiple-valued states. Thus, MVL device based on the vertical structures is not simply realized because some of the intermediate states may be degenerated.

From the technological view points, a large voltage difference between each spin orientation is indispensable for real applications. Normally, in the lateral spin devices, the induced voltage is not sufficiently large, typically in the range of a few microvolt by 1 mA. This is because the spin resistances of the ferromagnetic metals are much smaller than those of the nonmagnetic metals. However, by increasing the interface resistance using tunnel junction or increasing the spin polarization using Heusler ferromagnetic alloys, the spin resistance are effectively enhanced.^{8,9,16} When the spin resistance of the injector R_{SEI} and that of the detector R_{SED} are much larger than R_{SN} , the nonlocal spin voltage V is simply given by $V=(P_I P_D R_{SN} I_C / 2) \exp(-d/\lambda_N)$.¹³ In order to obtain a large spin voltage, the spin resistance for the nonmagnetic strip should be large with keeping the condition R_{SEI} and $R_{SED} \gg R_{SN}$. Since R_{SEI} and R_{SED} will be able to exceed 10 k Ω even in the ferromagnetic metals, it becomes possible to enlarge R_{SN} up to 1 k Ω . This leads to a large voltage generation (a few volt by 1 mA exciting current) even in the nonlocal geometry.

This work was supported by CREST from JST, NEDO, the Hosobunka, and the Mitsubishi Foundations.

¹J. Akerman, *Science* **308**, 508 (2005).

²M. Pakala, Y. Huai, T. Valet, Y. Ding, and Z. Diao, *J. Appl. Phys.* **98**, 056107 (2005).

³D. Weller, A. Moser, L. Folks, M. E. Best, W. Lee, M. F. Toney, M. Schwickert, J. U. Thiele, and M. F. Doerner, *IEEE Trans. Magn.* **36**, 10 (2000).

⁴K. C. Smith, *IEEE Trans. Comput.* **C-30**, 619 (1981).

⁵M. Johnson and R. H. Silsbee, *Phys. Rev. Lett.* **55**, 1790 (1985).

⁶F. J. Jedema, A. T. Filip, and B. J. van Wees, *Nature (London)* **410**, 345 (2001).

⁷T. Kimura, J. Hamrle, Y. Otani, K. Tsukagoshi, and Y. Aoyagi, *Appl. Phys. Lett.* **85**, 3501 (2004).

⁸S. O. Valenzuela and M. Tinkham, *Appl. Phys. Lett.* **85**, 5914 (2004).

⁹Y. Ji, A. Hoffmann, J. S. Jiang, and S. D. Bader, *Appl. Phys. Lett.* **85**, 6218 (2004).

¹⁰T. Kimura, J. Hamrle, and Y. Otani, *Phys. Rev. Lett.* **96**, 037201 (2006).

¹¹T. Yang, T. Kimura, and Y. Otani, *Nat. Phys.* **4**, 851 (2008).

¹²T. Kimura, J. Hamrle, and Y. Otani, *Phys. Rev. B* **72**, 014461 (2005).

¹³S. Takahashi and S. Maekawa, *Phys. Rev. B* **67**, 052409 (2003).

¹⁴T.-S. Kim, B. C. Lee, and H.-W. Lee, *Phys. Rev. B* **78**, 214427 (2008).

¹⁵T. Yang, A. Hirohata, T. Kimura, and Y. Otani, *Phys. Rev. B* **74**, 153301 (2006).

¹⁶Y. Fukuma, L. Wang, H. Idzuchi, and Y. Otani, *Appl. Phys. Lett.* **97**, 012507 (2010).